



Modified synthesis of nanoscale zero-valent iron and its ultrasound-assisted reactivity study on a reactive dye and textile industry effluents

Suvanka Dutta, Ananya Ghosh, Satarupa Satpathi, Rajnarayan Saha*

Department of Chemistry, National Institute of Technology, Durgapur 713209, West Bengal, India,
emails: suvanka.dutta@gmail.com (S. Dutta), virgo17sept@gmail.com (A. Ghosh), satarupasatpathi@gmail.com (S. Satpathi),
rnsahanitd@gmail.com (R. Saha)

Received 9 April 2015; Accepted 13 September 2015

ABSTRACT

Synthesized nanoscale zero-valent iron (NZVI) particles were applied for the degradation of a reactive dye Remazol Black B 133 and textile effluent. XRD and HR-TEM analysis of the synthesized particles showed body centered cubic crystal packing. The aggregates were spherical in shape and the size of the particles ranged from 5 to 15 nm. The reactive dye solution was substantially degraded by NZVI particles using ultrasonic irradiation under various experimental conditions created by varying NZVI dosages (0.15–0.30 g/L), initial dye concentration (25–200 mg/L), and pH (2–13). Experimental results suggest that NZVI particles work best within the pH range of 4–10. A unit gram of NZVI was found to degrade a maximum of 749.2 mg of RB B 133 dye and more than 80% of the dye was removed within 15 min of reaction time. During the degradation process, an oxidation–reduction potential change from 196 to –577 mV was detected, indicating reductive condition is necessary for effective dye removal. FT-IR analysis of the end products of the degradation process indicated the presence of an amino (–NH₂) group resulting from the breakdown of the azo (–N=N–) group. Results suggest that the degradation followed pseudo-first-order kinetics with respect to dye concentration. The effluents of two textile industries were collected, characterized, and treated with NZVI particles, which led to the significant fall below the standard scale of American Dye Manufacturing Institute (ADMI). This lowering of ADMI value indicates that the overall color removal efficiency is irrespective of any specific dye present in the effluent.

Keywords: NZVI; Open air synthesis; Reductive degradation; Remazol Black B 133 dye; Textile effluent

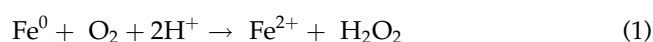
1. Introduction

Textile is one of the major industries of India, providing employment to over millions of people. But this industry leaves one of the largest water footprints on the planet, and dyeing poses an exceptionally big

problem which adds to the already existing problem of water pollution all over the world. Textile processing industry is characterized not only by the large volume of water required for different unit operations but also by the variety of chemicals used for various processes [1]. The effluents discharged from textile dyeing mills have high concentration of color. Major sources of effluent are intermediate washings carried

*Corresponding author.

out in between successive unit operations like bleaching, preparation for dyeing, etc.; among various kinds of dyes reactive dyes are the most widely used. In a reactive dye, the chromophore contains a substituent that reacts with the substrate clothing material and is most commonly used for dyeing cotton. They can also be applied on wool and nylon [2,3]. As most dyestuffs have complex aromatic groups in them that are resistant to degradation by biological wastewater treatment [4,5]. Dyes in the wastewater undergo chemical as well as biological decomposition, consume dissolved oxygen from the water bodies, and destroy aquatic life because of their toxicity [6]. There are many methods for dye removal like adsorption, coagulation/flocculation, ultrafiltration, reverse osmosis, ion exchange, membrane technology, and several other processes. All of these methods have their limitations, and none of them are successful in completely removing or degrading the colors from wastewater [7]. Nanoscale zero-valent iron (NZVI) has emerged as an efficient as well as cost-effective option for the treatment of contaminated soil and groundwater. When the NZVI particle size is extremely small, the particles develop high reducing ability and generate reactive oxygen species (ROS). ROS form from the transfer of energy or electrons to oxygen molecule. These ROS include species such as singlet oxygen, superoxide, hydrogen peroxide, and hydroxyl radical. Metallic or zero-valent iron, which is a two-electron donor through the redox pair of $\text{Fe}^{2+}/\text{Fe}^0$ with an E_0 of -0.44 V, can directly reduce dissolved molecular oxygen in aqueous solutions to hydrogen peroxide at its solid surface according to the well-studied iron corrosion theory [8]:



Hydrogen peroxide produced in the medium reacts with the metallic nanoparticles to form hydroxyl ions:



Free or surface-bound ferrous heterogeneously produced by reaction (1) or reaction (2) could then react with hydrogen peroxide or molecular oxygen via homogeneous or heterogeneous reactions to generate oxidants of hydroxyl radicals or ferryl-oxo complexes [9,10]. The particles being highly reactive (more reactive than granular iron which is conventionally applied in permeable reactive barriers for groundwater treatment) can be used for *in situ* remediation. NZVI particles effectively reduce phenolics, chlorinated organic contaminants (e.g. PCB, TCE, PCE,

phenol, pesticides, and solvents) [11–13], inorganic anions (ClO_4^- , SO_4^{2-} , PO_4^{3-} , and NO_3^-), etc. [14–16]. It can even be used to recover/remove dissolved heavy metals from solution (e.g. As(III), Cr(VI), U, and Pb) [17–21]. The reason behind the high reactivity of the nanoparticles can be attributed to the high specific surface area and the high surface energy of the nanoparticles. The physical and chemical effects of acoustic cavitation have been well documented over the last few decades [22]. The main reason behind the efficiency of ultrasonication is the cavitation phenomena that are accompanied by generation of local high temperature, pressure, and reactive radical species (HO^\bullet , HOO^\bullet) via thermal dissociation of water and oxygen [23]. Even more, ultrasonication increases transport of small molecules in a liquid solution by increasing the convection in an otherwise stagnant or relatively slow moving fluid [24]. The shockwave produced by the ultrasonic irradiation accelerated the NZVI particles to high velocities and disperse it homogeneously in the entire solution [25]. The combination of high power and longer sonication time can shorten the duration of the treatment process. Although for each special application of US, experimental results are needed to obtain the optimum power density, frequency, and irradiation time to reach a cost-effective and high application efficiency [23]. The model dye RB B 133 used for optimization of the degradation process commonly used in dyeing industry has discreet toxic significance. According to the material safety data sheet, this very dye is an equivocal tumorigenic agent and has bioaccumulation tendency. Carcinogenicity test on rats revealed that if exposed orally or subcutaneously, it can cause liver tumor, skin problems, and appendages (RTECS criteria) [26]. Though degradation of different types of dyes by NZVI particles have been reported in the literature, treatment of wastewater released from textile dye industries has been rarely reported. In the current work, not only aerobically synthesized stable NZVI particles were utilized, but the treatment was also enhanced by the assistance of ultrasonication. Moreover, this work aimed to establish a treatment method on a model dye and to run the process on actual textile effluents.

2. Materials and methods

2.1. Materials

Anhydrous FeCl_3 (Ferric Chloride), NaBH_4 (Sodium Borohydride), NaOH (Sodium Hydroxide),

Table 1
Particulars of the dye

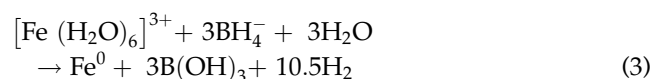
Name of the dye	Remazol Black B 133 (RB B 133)
Molecular formula	C ₂₆ H ₂₁ N ₅ Na ₄ O ₁₉ S ₆
Molecular weight	991.82
Chemical structure	
Chemical name	2,7-Naphthalenedisulfonic acid, 4-amino-5-hydroxy-3,6-bis[2-[4-[[2(sulfooxy)ethyl]sulfonyl]phenyl]diazenyl]-, sodium salt
CI No.	20505
CAS No.	17095-24-8

and HCl (Hydrochloric acid) were purchased by Merck India Pvt. Ltd. Particulars of the dye are given in Table 1. All the chemicals were used as received, without further purification.

2.2. Synthesis of NZVI under aerobic conditions

NZVI particles were synthesized by bottom-up approach using ethanol–water system without maintaining the inert conditions and modifying the reference method [27,28]. Ethanol was chosen because of its hygroscopic nature and its higher dissolved oxygen solubility, so addition of ethanol causes a reduction in oxidation of the nanoparticles by forming a protective layer on the outer sphere of the nanoparticles. Moreover, other researches already established that ethanol can serve both as solvent and reducing agent [29]. Reduction of ethanol is a two-step process, in the first step acetaldehyde is formed and in the second step it is further reduced to acetic acid. It is also noted that the intermediate acetaldehyde is less stable, and is a stronger reductant than ethanol [30]. Though the reduction potential of ethanol–water system is not enough for reduction of Fe³⁺ to Fe⁰ ($E^0 = -0.04$ V vs. SHE), it can maintain an effective reducing environment to prevent further oxidation of Fe⁰ in open air [28]. During the synthesis process, 0.067(M) FeCl₃ (anhydrous) was prepared with ethanol/water (4:1) mixture and stirred well. 0.1 M sodium borohydride

solution was prepared and was added drop by drop into the iron(III) chloride solution placed in a 500-mL conical flask at room temperature. After the synthesis was over, the nanoparticles were washed with ethanol, and the particles were dried in a vacuum oven at a temperature of 60°C. The particles were then collected and stored in a vacuum desiccator for future use. The reaction scheme is as shown in Eq. (3):



2.3. Experimental procedure

A 1,000 mg/L stock solution of dye RB B 133 (1,000 mg) was precisely prepared in milipore (18 mΩ) water. From the stock solution five known standards were prepared and their corresponding absorbance was noted at λ_{max} (595 nm). The plot of absorbance vs. concentration gives a straight line having a slope value of 31.06. This calibration curve was used to determine dye concentrations in samples. Different intermediate solutions (25–200 mg/L) were prepared from the stock solution and charged into the reactor at a mixing rate of 300 rpm, taking into consideration the time (up to 60 min) and dosages of NZVI (0.15–0.30 g/L) and pH (2–12). The initial pH only was adjusted by (0.1 N and 1 N) HCl or (0.1 N and 1 N)

NaOH and measured using an Orion star A214 Thermo Scientific pH meter. All the reactions were carried out in a Rivotek ultrasonic cleaning bath at 30 ± 3 kHz. The ultrasonic cleaner had an output power of 50 W and an electric supply of 230 V/50 Hz AC, single phase. The tank dimensions were $225 \text{ mm} \times 125 \text{ mm} \times 60 \text{ mm}$ with a liquid-holding capacity of 1.5 L. At defined time intervals, water samples were withdrawn and the dye concentrations were calculated by measuring the absorbance at 595 nm using a double beam UV–vis spectrophotometer (SHIMADZU UV-1601). All the experiments were triplicated and the mean values represent the main points of the graphs, whereas standard deviation was represented by the error bars. The oxidation–reduction potential (ORP) were monitored by Orion 420+ ion meter with specific probes. For the IR data, Thermo NICOLET iS10 FTIR instrument was used. Temperature was adjusted to $35 \pm 2^\circ\text{C}$ manually throughout the experiment within the ultrasonic bath by adding room temperature water and removing comparatively warm water from the bath. As the synthesis and treatment were both performed without maintaining anaerobic condition, effect of the dissolved oxygen was not taken into account separately.

2.4. Characterization of the zero-valent iron nanoparticles

Images of NZVI particles were recorded in TECHNAI TF20 ST High Resolution Transmission Electron Microscope (HRTEM) operated at 200 kV. The sample was dispersed in ethanol prior to the grid preparation. 2–3 drops of the dilute ethanol solution of the sample were then added onto a copper grid. The samples were then put in a vacuum hood till the ethanol evaporated completely. XRD analysis was conducted by PAN ANALYTICAL XPERT PRO diffractometer. It used copper $K\alpha$ radiation and a graphite monochromator to produce X-rays of wavelength 1.54 \AA . The nanoparticles were placed in a glass sample holder and scanned in the range of 35° – 105° . This range covered all the species of iron and iron oxides [31,32].

2.5. characterization of textile effluent and description of the study area

All water parameters of textile effluent were measured as per the standard method of APHA [33]. The color intensity of the effluent was analyzed by American Dye Manufacturers Institute (ADMI) standard color measurement by applying the Adams–Nickerson color difference formula following Method

2120E of the Standard Methods [33]. The study area is located at Boda Panchayet, Jugberia, Sodepur in West Bengal, India. The geographical location of the sampling area is $22^\circ 41' 45.17''$ North and $88^\circ 23' 42.67''$ East. Effluents were collected from two small-scale textile dyeing industries “Sanjay limited” and “Annappurna Textile Limited”.

3. Result and discussion

3.1. Particle characterization

Fig. 1 shows the HR-TEM images of the iron nanoparticles. The shape of the nanoparticles was mostly spherical with particles in the range of 5–15 nm. A sharp peak at 44.67° (2θ) in the XRD image (Fig. 2) revealed that the particles formed were crystalline in nature. This is the characteristic peak for zero-valent iron nanoparticles. Crystallite size of NZVI is obtained from Debye Scherrer equation (Eq. (4)). The calculated value of crystallite particle is 13 nm

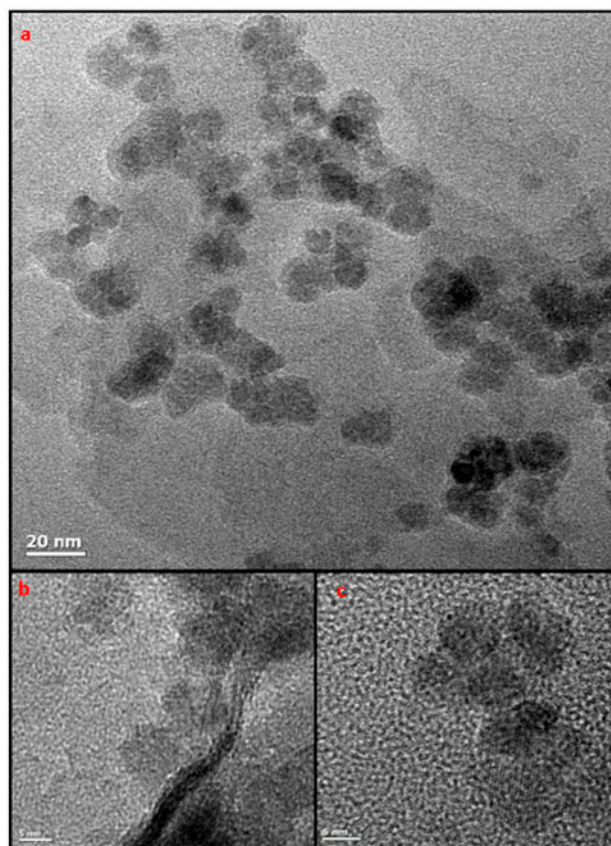


Fig. 1. HR-TEM images (a–c) of the synthesized zero-valent iron nanoparticles.

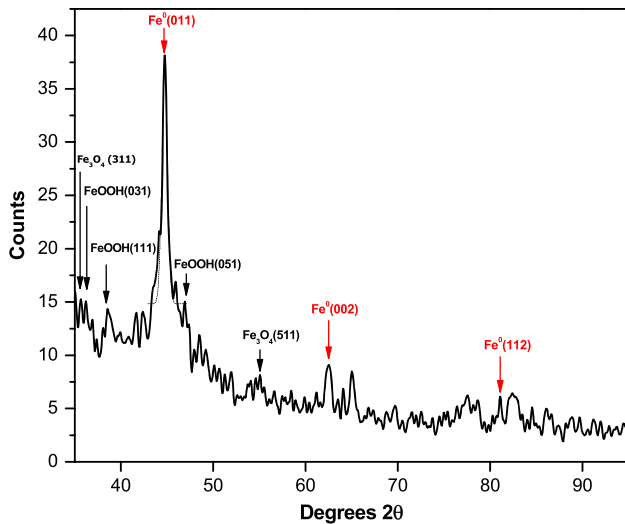


Fig. 2. X-ray diffraction image of the synthesized iron particles.

which is in accordance to the size obtained from HR-TEM image.

$$t = \frac{k\lambda}{\beta \cos \theta} \quad (4)$$

Here t = crystallite size (nm), k = constant (0.9), λ = X-ray wave length in nm (Cu lamp = 1.54 nm), θ = Diffraction angle ($2\theta = 44.74$), and β = Full Width Half Maximum (FWHM) in radian (0.0109 rad). The particle size here is less than most of the previously reported scientific articles. Yuvakkumar et al. [28] reported 50–100 nm particle diameter in his open air synthesis method. Less than 100 nm particles were synthesized by Satapanajaru et al. [34]. The unit cell of the crystalline particles was body-centered cubic (bcc) having α phase (concluded after comparing data with ICSD data ref. code 98-002-1567). The coordination number of the surface layer atoms for the bcc lattice is six. Each surface atom has four nearest neighbors in the first layer (the remaining two “near-neighbors” in this surface layer being at a slightly greater distance), but there are also two nearest neighbors in the layer immediately below. The coordination number of an atom in the bulk bcc unit cell being eight makes the surface energy high and the nanoparticles highly reactive. Also the specific surface area which is inversely proportional to the diameter of the nanoparticles increases a lot as the size of the nanoparticles decreases to the range of 5–15 nm (approx.). Both these factors lead to high reaction efficiency of NZVI.

3.2. Effects on initial dye concentration over time during the degradation

In aqueous medium, NZVI particles dissociate into ferrous ions, thereby releasing two electrons. The released electrons can rapidly combine with certain organic compounds present in the medium (in this case “Azo Reactive dye RB B 133”), resulting in reduction of the organic concentrations. In earlier research work, it was already established that NZVI mainly breaks down the dye via reductive degradation [35] of the azo group of the dye molecule. Introduction of ultrasonication in the current work individually, hardly affects the dye degradation process. As the control experiment (Fig. 3) shows, the presence of NZVI ultrasonication enhances the degradation with respect to mechanical stirring of reaction medium.

NZVI being magnetic in nature has a great tendency to get agglomerated due to the magnetic forces of attraction, application of ultrasonication throughout the experiments reduces this very tendency of agglomeration thereby increasing the exposure of reactive surface area of the nanoparticles. Ultrasonication increases the dispersion of NZVI by the basic mechanism of transporting small molecules/aggregates in a liquid solution by increasing the convection in an otherwise stagnant or relatively slow moving fluid [24]. Many researchers previously demonstrated that the azo bond (N=N) in dyes such as Acid Orange 2 [35], Acid Blue 113 [36], Acid Red 14, Acid Red 18 [37], Reactive Black 5, and Reactive Red 198 [38] was degraded by zero-valent iron. Similar observation was made in case of color removal in terms of ADMI value (Fig. 4).

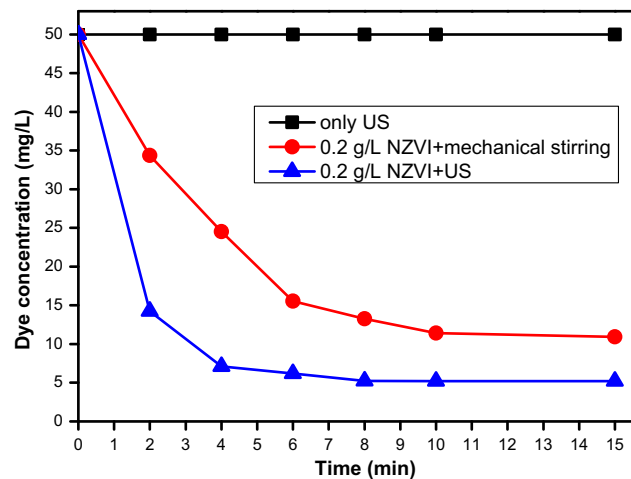


Fig. 3. Control experiments of treatment (50 mg/L dye solution): using only ultrasonication; NZVI and mechanical stirring; NZVI and ultrasonication together.

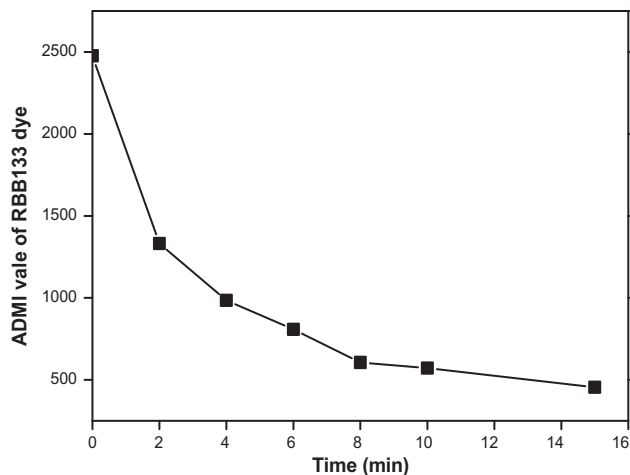


Fig. 4. Change of ADMI value with respect to time during the treatment process of RB B 133 dye.

Within the first fifteen minutes effective dye removal was noted. This is because the azo (N=N) bonding of dye molecules responsible for the absorbance of color was cleaved resulting in dye concentration as well as color removal. For a 50 mg/L initial dye concentration, a removal efficiency of about 79% was found after the first 2 min and 98% within 15 min. Marginal removal was observed afterward. After addition of 0.2 g/L NZVI particles, the RB B 133 dye concentration reduction curves vs. time are shown in Fig. 5 at different initial dye concentrations. It can be seen that irrespective of the dye concentration, the degradation was initially very sharp and then remained moderately slow.

Besides time, the initial dye concentration and NZVI dosages were the other factors studied for dye

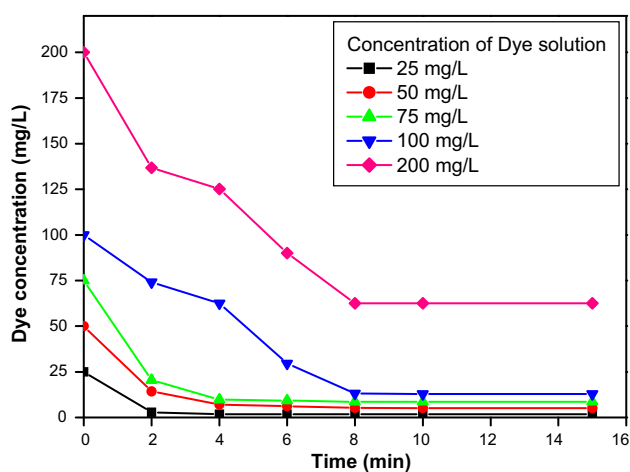


Fig. 5. Residual dye (RB B 133) concentrations during the treatment process with NZVI.

removal capacity. The effect of the NZVI dose shown in Fig. 6 indicates that RB B 133 dye degradation efficiency increased with the increase in the NZVI dosages. So the dye concentration varied from 25 to 200 mg/L and NZVI doses from 0.15 to 0.3 g/L. Increasing the dose of NZVI provided substantially more active surface sites to accelerate the initial reaction. This resulted in more NZVI surface collisions with a greater number of RB B 133 dye molecules to enhance its degradation. For 200 mg/L RB B 133 dye solution, degradation efficiencies of 66.2, 68.7, 76.5, and 88.6% were obtained (Fig. 6) for NZVI dosages of 0.15, 0.2, 0.25, and 0.3 g/L over 60 min, respectively. The effect of unit amount of NZVI load on dye degradation and also its relationship to removal efficiency is shown in Fig. 7.

It is apparent that the unit NZVI dye removal capacities (URCs) are the function of NZVI load (0.15–0.3 g/L). The URCs are found to be 883, 687, 612, and 590 mg of RB B 133 dye/g NZVI for NZVI dose of 0.15, 0.2, 0.25, and 0.3 g/L and for initial dye concentration of 200 mg/L over the course of 60 min. The higher NZVI dose gave higher dye removal; nevertheless, they provided lower URCs at the same initial dye concentration. From Fig. 7 it can be seen

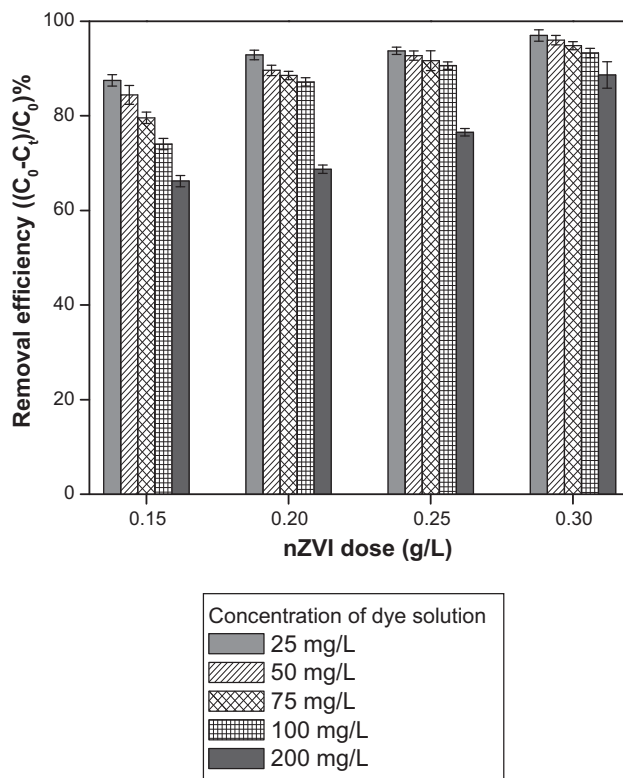


Fig. 6. Dye removal efficiency of RB B 133 dye with respect to various Dye concentrations and NZVI dosages.

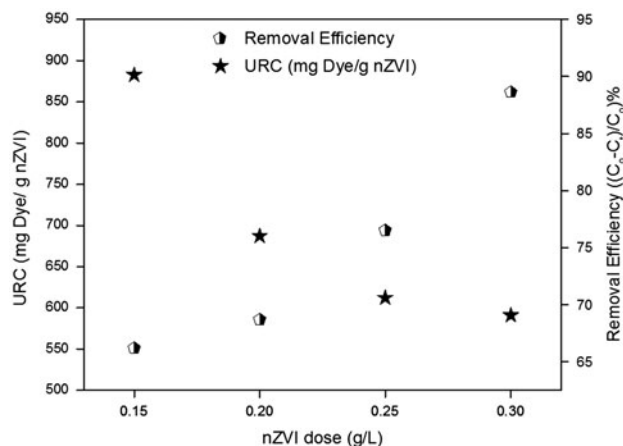


Fig. 7. Relationship between unit removal capacity (URC) and Dye removal efficiency.

that above NZVI dosage of 0.25 g/L, the URC values reach saturation. Increasing the NZVI dosage beyond this value has little effect on URC.

3.3. Effect on pH and ORP

While monitoring the reaction for 30 min, the ORP dropped from 196 to -406.5 mV rapidly, and then gradually decreased to -577 mV. Later the value increased to -430 mV at 90 min. This indicates reductive conditions for effective dye removal within the first 15 min. Within the NZVI reaction system there are several factors which play a vital role in lowering the ORP value. Along with consumption of reducible contaminant and removal of oxygen, generation of $\text{Fe}^{(2+)}/\text{Fe}^{(3+)}$ species and H_2 evolution are the main reasons behind the drop in ORP [39]. Moreover, pH variation was also detected during reduction. The pH raised sharply from 2.5 to 7.6 in the initial 6 min, and then increased very slowly to 8.1 with time (Fig. 8). The pH change in the first 6 min can be attributed to NZVI dissolution: NZVI spontaneously reacts with water molecules to release hydroxyl ions which increase the pH from 2.5 to 8. Similar findings were also observed by Shu et al. [40,41].

3.4. Effect of pH

pH is also one of the important factors controlling dye removal rate by NZVI. When the ferrous ions dissolve out from the iron surface and collide with hydroxyl ions present in the reaction medium, ferrous hydroxide is precipitated on the iron surface thus occupying the reactive sites to hinder the reaction [40]:

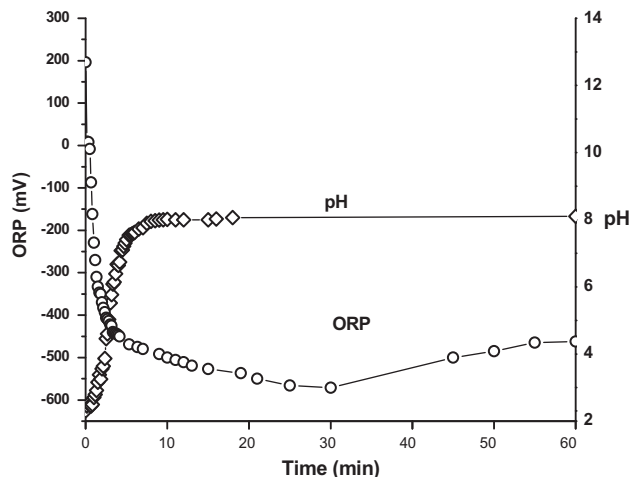
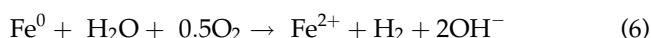
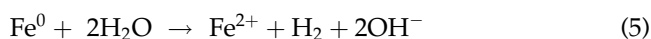


Fig. 8. Change of pH and ORP values with time during dye degradation treatment process.



This means that acidic conditions favor reduction process. The effect of pH on 50 mg/L RB B 133 dye removal on addition of 0.2 g/L NZVI is illustrated in Fig. 9. The pH of the original solution was 7.03. Around the range of pH 4–9, more than 80% of dye removal was observed. Extremely basic or acidic conditions gave poor removal; for example, adding sodium hydroxide solution (1.0 M) to elevate pH to 13 or hydrochloric acid (1.0 M) to drop pH to 2 significantly reduced the RB B 133 dye removal efficiency from the original pH conditions. Low pH range may remove the passivating layers off the NZVI core [32,40,42], rendering the nanoparticles free to react with the azo group in the dye molecules. This result may also be ascribed to the pH_{zpc} (zero point charge) of NZVI. Li et al. [43] indicated that the pH_{zpc} of NZVI is around 8. At a low pH (pH_{zpc}), the NZVI surface has positive charge, and the dye molecules, with a negative charge bearing SO_3^- group [44], attract the NZVI particles toward themselves. Thus, the degradation reaction between the dye molecules and NZVI could be achieved easily. On the other hand, at an alkaline pH, the zero-valent iron surface might be covered with corrosion products formed under these conditions. This phenomenon causes a lowering of the reducing power of NZVI and mass transport limitations on NZVI surface. The charge of the surface also changes from positive to negative with an increase in solution pH [45].

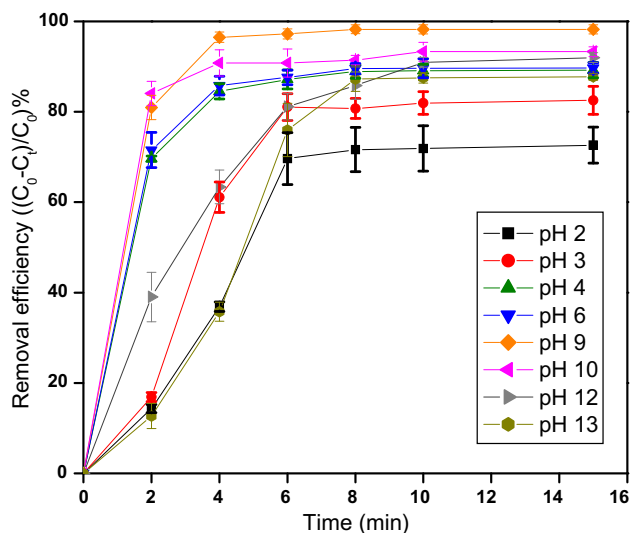


Fig. 9. Removal efficiency of RB B 133 dye during treatment with NZVI at different pHs.

3.5. Kinetics study

In this dye degradation process, a first-order reaction is generally assumed with respect to dye concentration. It converts into a pseudo-first-order reaction ignoring NZVI particle concentration effects, as:

$$C_{\text{dye}} = C_{\text{dye}}^0 \times e^{-kt} \quad (7)$$

where k denotes the observed first-order reaction rate constant (min^{-1}), t the reaction time (min), C_{dye}^0 the initial concentration (mg/L) of RB B 133, and C_{dye} is the concentration (mg/L) of RB B 133 at time t . The removal efficiency hardly reaches to 100% completion due to the limited transfer between water and the NZVI particle inter-phase, so the residual dye concentration can be expressed by the proposed empirical rate equation:

$$C_{\text{dye}} = C_{\text{ultimate}} + (C_{\text{dye}}^0 - C_{\text{ultimate}}) \times \alpha \times e^{-kt} \quad (8)$$

where C_{ultimate} is the ultimate residual dye concentration (mg/L) for a certain NZVI dose (g/L), α denotes the variation coefficient (1.0 denotes ideal first-order kinetic, the larger the deviation from 1.0 the less fit the first-order kinetics) of removed dye concentration for each test and k denotes the empirical rate constant (min^{-1}) [40,41,46]. The constants C_{ultimate} , α , and k were obtained by linear regression. The whole study was performed with 50 mg/L dye solution with 0.2 g/l NZVI dosage at different pHs. Table 2 summarizes rate

Table 2

Result of regression analysis of experimental data of RB B 133

C_{ultimate} (mg/L)	pH	α	k (min^{-1})	R^2
13.67	2	0.21	0.73	0.942
8.73	3	0.24	0.79	0.947
5.39	4	1.16	0.66	0.988
5.14	6	1.27	0.68	0.958
0.87	9	1.6	0.71	0.891
3.34	10	1.18	0.33	0.759
4.00	12	1.82	0.47	0.957
6.13	13	0.13	0.80	0.929

constants from all the different experiments performed. The experimental results (Table 2) show that α value of pH 2, 3, 12, and 13 give the higher deviations from 1 indicating that the degradation at these pHs does not follow first-order reaction.

3.6. FTIR analysis of dye degradation

FT-IR analysis was done for the dye and their degraded products. The degraded products of the dyes were separated based on their solubility in water and methanol.

RB B 133 dye and its degraded products: In case of RB B 133 dye before treatment, the stretching frequencies was observed at 3455 cm^{-1} (ν_{OH}), 3380 cm^{-1} (ν_{NH}), 2850 cm^{-1} (ν_{CH}), 1502 cm^{-1} (ν_{NN}), and 1052 cm^{-1} (ν_{SO}) (Fig. 10(a)). Degradation of the

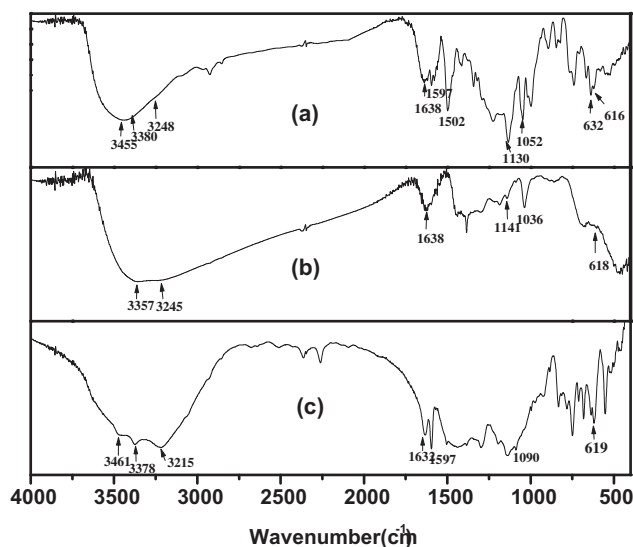


Fig. 10. FTIR study of RB B 133 dye before and after the treatment (a) RB B 133 dye, (b) water insoluble degraded products, and (c) water soluble degraded products.

dye by NZVI gives rise to two amines by the breakage of the azo bond, which were separated by solubility in two different solvents, water, and methanol. After treatment with NZVI, the degraded products do not display stretch at $1,502\text{ cm}^{-1}$ (ν_{NN}) but few new stretches appeared at $3,357, 3,245\text{ cm}^{-1}$ (Fig. 10(b)), and $3,378, 3,215\text{ cm}^{-1}$ (Fig. 10(c)) for corresponding primary amines which may corroborate by breaking the $\text{N}=\text{N}$ bond during the treatment with NZVI. On the other hand, the water insoluble and methanol soluble parts do not show stretching frequency for OH group. The IR spectra of the selected dye before and after treatment with NZVI are given in Fig. 10. Therefore, it may be concluded that the selected dye undergoes cleavage of azo bond present in the parent dye during the treatment with NZVI.

3.7. Characterization and study of industrial dye effluent degradation collected from the industrial area

The general characteristics of the dye effluent collected from the discharge channel of two industries are given in the following table.

As the concentration of the dyes present in these two different effluents is unknown, the degradation study was done by taking a scan of the total absorption spectra and then calculating the ADMI value. From the graph it can be said that just by filtration of the effluent, the color intensity is removed by more than 50% (Figs. 11(a) and 12(a)). This fact can be attributed to the presence of huge amount of TSS in both the effluents (Table 3). The fluffy cotton and wool

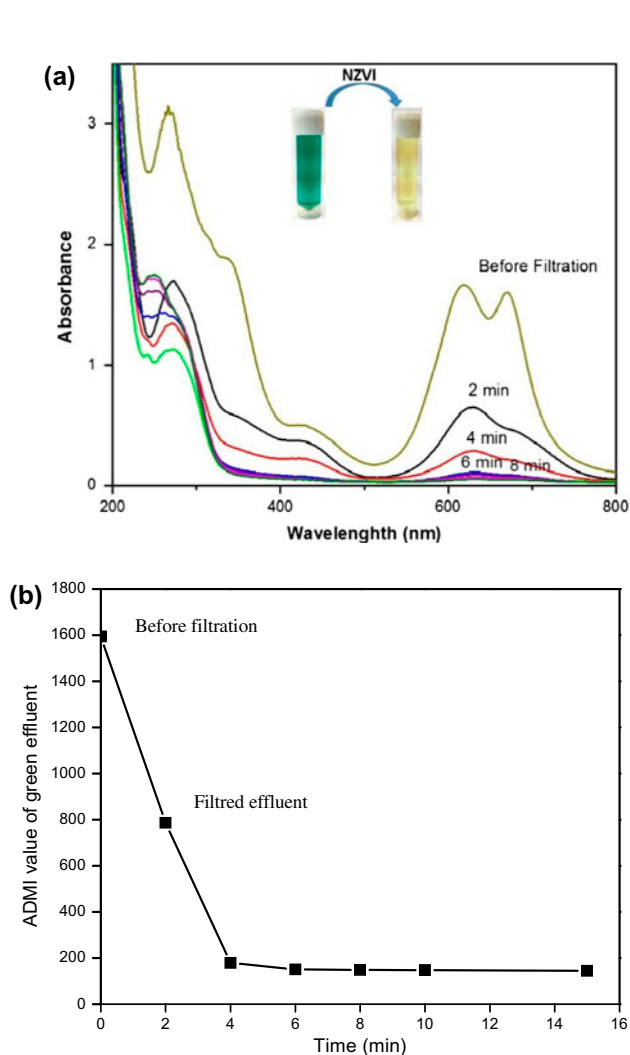


Fig. 11. Study of absorbance spectra (a) and ADMI (b) value during the treatment process of effluent of Sanjay limited.

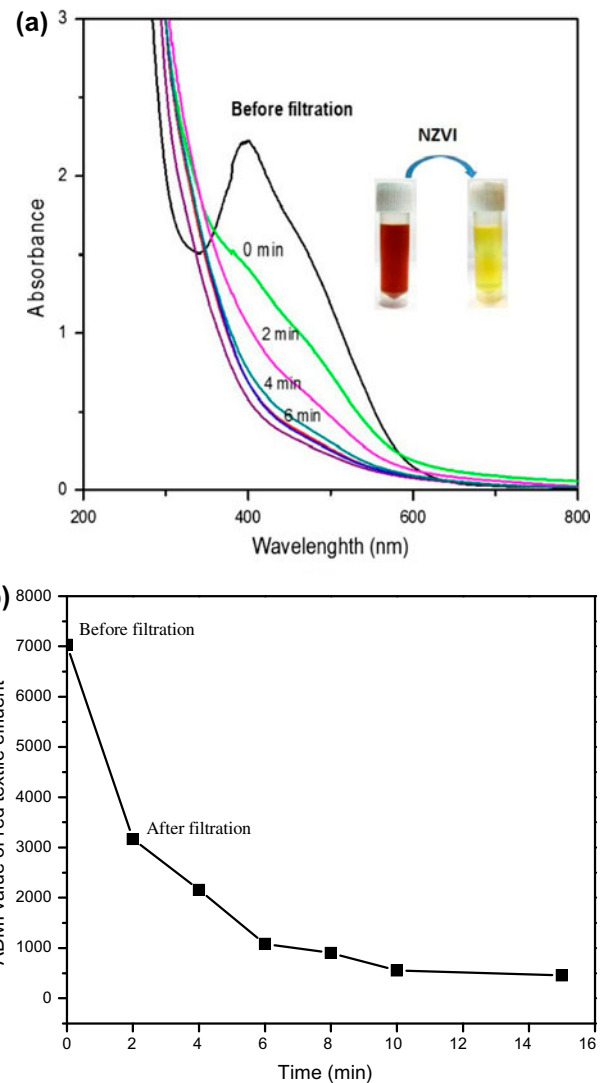


Fig. 12. Study of absorbance spectra (a) and ADMI value (b) during the treatment process.

Table 3
General characterization of textile effluents collected from textile industries

Parameters	Annapurna textile limited (Red effluent)	Sanjay limited (Green effluent)
pH	12.5	8.52
EC (μS)	197	112
Temperature ($^{\circ}\text{C}$)	65	71.5
TDS (mg/L)	108	44.8
TSS (mg/L)	2,708	674
ORP (mV)	−90	114
Chloride (mg/L)	2,150	2,700
ADMI	7,032	1,594.3

mass generates the suspended solid and it absorbs the spent dye. The filtration decreases the ADMI value for the effluent from Sanjay limited (Fig. 11(b)) from 1,600 to near 800 and for the effluent from Annapurna Textile Limited (Fig. 12(b)), ADMI value is reduced to around 3,000 from 7,000. Then after, the treatment with NZVI, the ADMI value is reduced to less than 500. As the pH of the effluent from Annapurna Textile Limited is 12.5, the degradation with NZVI becomes slow and takes more than 10 min to remove the color of the effluent with a dose of 0.3 g/L NZVI. On the other hand the effluent from Sanjay limited with a pH of 8.5, degrades sharply on addition of 0.2 g/L NZVI. So from this study, it is established that the degradation with NZVI is highly pH dependent, as the observation is in accordance with the earlier result of synthetic dye solution.

4. Conclusion

From the characterization data it can be concluded that the aerobic method of synthesis developed, can produce particles within 5–15 nm. RB B 133 dye and textile dye effluents can be effectually reduced in aqueous solution with NZVI particles. The reactions were affected by NZVI dosages, initial dye concentrations, and pH. Major percentage of the dye degraded within 15 min of NZVI addition, irrespective of the pH conditions. The empirical equation for the kinetics study shows that the experimental data of pH 4–10 were well fitted into first-order reaction rate equation. The FT-IR study detected the presence of corresponding amines of the dye as the products of degradation. The color intensity (ADMI value) of the dye effluent from the textile industries was also reduced from 800 to 200 for the effluent from Sanjay Limited, and for Annapurna Textile Limited it was reduced from 3,000 to less than 500. These data support the fact that NZVI is a fast and efficient remedy for environmental contamination.

Acknowledgments

We like to acknowledge National Institute of Technology Durgapur, for providing infrastructure. Great assistance provided by our fellow research scholars Ram Chandra Maji, Sanjit Saha, and Humayun Kabir.

References

- [1] K. Rajeswari, R. Subashkumar, K. Vijayaraman, Biodegradation of mixed textile dyes by bacterial strains isolated from dye waste effluent, *Res. J. Environ. Toxicol.* 5 (2011) 97–107.
- [2] B. Manu, S. Chaudhari, Decolorization of indigo and azo dyes in semicontinuous reactors with long hydraulic retention time, *Process Biochem.* 38 (2003) 1213–1221.
- [3] H.Y. Shu, C.R. Huang, M.C. Chang, Decolorization of mono-azo dyes in wastewater by advanced oxidation process: A case study of acid red 1 and acid yellow 23, *Chemosphere* 29 (1994) 2597–2607.
- [4] H. Tappe, W. Helmling, P. Mischke, K. Rebsamen, U. Reiher, W. Russ, L. Schläfer, P. Vermehren, Reactive dyes, *Ullmann's Encyclopedia of Industrial Chemistry*, 2000, doi: 10.1002/14356007.a22_651.
- [5] M.N. Ahmed, R.N. Ram, Removal of basic dye from waste-water using silica as adsorbent, *Environ. Pollut.* 77 (1992) 79–86.
- [6] P.A. Carneiro, G.A. Umbuzeiro, D.P. Oliveira, M.V. Zononi, Assessment of water contamination caused by a mutagenic textile effluent/dyehouse effluent bearing disperse dyes, *J. Hazard. Mater.* 174 (2010) 694.
- [7] P. Prema, S. Thangapandian, M. Selvarani, S. Subharanjani, Color removal efficiency of dyes using nanozerovalent iron treatment, *Toxicol. Environ. Chem.* 93(10) (2011) 1908–1917.
- [8] S.H. Joo, A.J. Feitz, D.L. Sedlak, T.D. Waite, Quantification of the oxidizing capacity of nanoparticulate zero-valent iron, *Environ. Sci. Technol.* 39 (2005) 1263–1268.
- [9] H. Wu, J.J. Yin, W.G. Wamer, M. Zeng, Y.M. Lo, Reactive oxygen species-related activities of nano-iron metal and nano-iron oxides, *J. Food Drug Anal.* 22 (2014) 86–94.
- [10] S. Zecevic, D.M. Drazic, S. Gojkovic, Oxygen reduction on iron: Part III. An analysis of the rotating disk-

- ring electrode measurements in near neutral solutions, *J. Electrochem. Soc.* 265(1–2) (1989) 179–193.
- [11] Q. Wang, S.W. Jeong, H. Choi, Removal of trichloroethylene DNAPL trapped in porous media using nanoscale zerovalent iron and bimetallic nanoparticles: Direct observation and quantification, *J. Hazard. Mater.* 213–214 (2012) 299–310.
- [12] A. Shimizu, M. Tokumura, K. Nakajima, Y. Kawase, Phenol removal using zero-valent iron powder in the presence of dissolved oxygen: Roles of decomposition by the Fenton reaction and adsorption/precipitation, *J. Hazard. Mater.* 201–202 (2012) 60–67.
- [13] G.V. Lowry, S.A. Majestic, K. Matyjaszewski, R.D. Tilton, Final Report: Developing Functional Fe(0)-based Nanoparticles for In Situ Degradation of DNAPL Chlorinated Organic Solvents, Carnegie Mellon University, 2007. Available from: <<http://www.ce.cmu.edu/~glowry/>>.
- [14] D. Wu, Y. Shen, A. Ding, M. Qiu, Q. Yang, S.H. Zheng, Phosphate removal from aqueous solutions by nanoscale zero-valent iron, *Environ. Technol.* 34(18) (2013) 2663–2669.
- [15] J. Xu, Z. Hao, C. Xie, X. Lv, Y. Yang, X. Xu, Promotion effect of Fe²⁺ and Fe₃O₄ on nitrate reduction using zero-valent iron, *Desalination* 284 (2012) 9–13.
- [16] Y. Zhang, Y. Li, J. Li, L. Hub, X. Zheng, Enhanced removal of nitrate by a novel composite: Nanoscale zero valent iron supported on pillared clay, *Chem. Eng. J.* 171 (2011) 526–531.
- [17] X. Zhang, Shen Lin, Z. Chen, M. Megharaj, R. Naidu, Kaolinite-supported nanoscale zero-valent iron for removal of Pb²⁺ from aqueous solution: Reactivity, characterization and mechanism, *Water Res.* 45 (2011) 3481–3488.
- [18] C. Wang, H. Luo, Z. Zhang, Y. Wu, J. Zhang, S. Chen, Removal of As(III) and As(V) from aqueous solutions using nanoscale zero valent iron-reduced graphite oxide modified composites, *J. Hazard. Mater.* 268 (2014) 124–131.
- [19] K.P. Kowalski, E.G. Søgaard, Implementation of zero-valent iron (ZVI) into drinking water supply—Role of the ZVI and biological processes, *Chemosphere* 117 (2014) 108–114.
- [20] S. Klimkova, M. Cernik, L. Lacinova, J. Filip, D. Jancik, R. Zboril, Zero-valent iron nanoparticles in treatment of acid mine water from *in situ* uranium leaching, *Chemosphere* 82(8) (2011) 1178–1184.
- [21] X. Lv, Y. Hu, J. Tang, T. Sheng, G. Jiang, X. Xu, Effects of co-existing ions and natural organic matter on removal of chromium (VI) from aqueous solution by nanoscale zero valent iron (nZVI)-Fe₃O₄ nanocomposites, *Chem. Eng. J.* 218 (2013) 55–64.
- [22] K.P. Gopinath, K. Muthukumar, M. Velan, Sonochemical degradation of Congo red: Optimization through response surface methodology, *Chem. Eng. J.* 157 (2010) 427–433.
- [23] M.R. Doosti, R. Kargar, and M.H. Sayadi, Water treatment using ultrasonic assistance: A review, *Proc. Int. Acad. Ecol. Environ. Sci.* 2(2) (2012) 96–110.
- [24] W.L. Nyborg, Biological effects of ultrasound: Development of safety guidelines. Part II: General review, *Ultrasound Med. Biol.* 27(3) (2001) 301–333.
- [25] M.R. Taha, Characterization of nano zero-valent iron (nZVI) and its application in sono-Fenton process to remove COD in palm oil mill effluent, *J. Environ. Chem. Eng.* 2(1) (2014) 1–8.
- [26] Remazol Black B 133. MSDS NO: 306452, Sigma Aldrich. Available from: <<http://www.sigmaaldrich.com/MSDS/MSDS/DisplayMSDSPage.do?country=IN&language=en&productNumber=306452&brand=SIAL&PageToGoToURL=http%3A%2F%2Fwww.sigmaaldrich.com%2Fcatalog%2Fproduct%2F306452%3F3Den>>.
- [27] W. Wang, Z.H. Jin, T.L. Li, H. Zhang, S. Gao, Preparation of spherical iron nanoclusters in ethanol–water solution for nitrate removal, *Chemosphere* 65(8) (2006) 1396–1404.
- [28] R. Yuvakkumar, V. Elango, V. Rajendran, N. Kankan, Preparation and characterization of zero valent iron nanoparticles, *Digest J. Nanomater. Biostruct.* 6(2011) 1771–1776.
- [29] A. Pal, S. Shah, S. Devi, Microwave-assisted synthesis of silver nanoparticles using ethanol as a reducing agent, *Mater. Chem. Phys.* 114 (2009) 530–532.
- [30] J.X. Wang, US Patent 20130264198 A1, Washington, DC, U.S. Patent and Trademark Office.
- [31] X. Li, D.W. Elliott, W. Zhang, Zero-valent iron nanoparticles for abatement of environmental pollutants: Materials and engineering aspects, *Crit. Rev. Solid State Mater. Sci.* 31 (2006) 111–122.
- [32] Y.P. Sun, X.Q. Li, J. Cao, W.X. Zhang, H.P. Wang, Characterization of zero-valent iron nanoparticles, *Adv. Colloid Interface Sci.* 120 (2006) 47–56.
- [33] L.S. Clesceri, A.E. Greenberg, A.D. Eaton, Standard Methods for the Examination of Water and Wastewater, 20th ed., American Public Health Association, Washington, DC, 1998, pp. 4–11.
- [34] T. Satapanajaru, C. Chompuchan, P. Suntornchot, P. Pengthamkeerati, Enhancing decolorization of Reactive Black 5 and Reactive Red 198 during nano zerovalent iron treatment, *Desalination* 266 (2011) 218–230.
- [35] J. Cao, L. Wei, Q. Huang, L. Wang, S. Han, Reducing degradation of Azo dyes by zero-valent iron in aqueous solution, *Chemosphere* 38(3) (1999) 560–565.
- [36] S. Nam, P.G. Tratnyek, Reduction of azo dyes with zero-valent iron, *Water Res.* 34(6) (2000) 1837.
- [37] M.R. Samarghandi, M. Zarrabi, A. Amrane, M.N. Sepehr, M. Noroozi, S.A. Namdari, Kinetic of degradation of two azo dyes from aqueous solutions by zero iron powder: Determination of the optimal conditions, *Desalin. Water Treat.* 40 (2012) 137.
- [38] C. Chompuchan, T. Satapanajaru, P. Suntornchot, P. Pengthamkeerati, Decolourization of Reactive Black 5 and Reactive Red 198 using nanoscale zero valent iron, *World Acad. Sci. Eng. Technol.* 49 (2009) 94–98.
- [39] Z. Shi, J.T. Nurmi, P.G. Tratnyek, Effects of nano zero-valent iron on oxidation–reduction potential, *Environ. Sci. Technol.* 45 (2011) 1586–1592.
- [40] H.Y. Shu, M.C. Chang, C.C. Chang, Integration of nano-sized zero-valent iron particles addition with UV/H₂O₂ process for purification of azo dye Acid Black 24 solution, *J. Hazard. Mater.* 167 (2009) 1178–1184.
- [41] H.Y. Shu, M.C. Chang, H.H. Yu, W.H. Chen, Reduction of an azo dye Acid Black 24 solution using synthesized nanoscale zerovalent iron particles, *J. Colloid Interface Sci.* 314 (2007) 89–97.

- [42] T. Satapanajaru, P. Anurakpongsatorn, P. Pengthamkeerati, H. Boparai, Remediation of atrazine-contaminated soil and water by nano zerovalent iron, *Water Air Soil Pollut.* 192 (2008) 349–359.
- [43] Z. Li, H.K. Jones, P. Zhang, R.S. Bowman, Chromate transport through columns packed with surfactant-modified zeolite/zero valent iron pellets, *Chemosphere* 68 (2007) 1861–1866.
- [44] J. Fan, Y. Guo, J. Wang, M. Fan, Rapid decolorization of azo dye methyl orange in aqueous solution by nanoscale zerovalent iron particles, *J. Hazard. Mater.* 166 (2009) 904–910.
- [45] W. Stumm, B. Sulzberger, J. Sinniger, The coordination chemistry of the oxide-electrolyte interface—The dependence of the surface reactivity (dissolution, redox reactions) on surface structure, *Croat. Chem. Acta.* 63 (1990) 277–312.
- [46] H.Y. Shu, M.C. Chang, C.C. Chen, P.E. Chen, Using resin supported nano zero-valent iron particles for decoloration of Acid Blue 113 azo dye solution, *J. Hazard. Mater.* 184 (2010) 499–505.